# Electroweak Corrections to the Charged Higgs Boson Decay into Chargino and Neutralino *

Wan Lang-Hui[b], Ma Wen-Gan[a,b],Zhang Ren-You[b], and Jiang Yi[b]
[a] CCAST (World Laboratory), P.O.Box 8730, Beijing 100080,P.R.China
[b] Department of Modern Physics, University of Science and Technology of China (USTC), Hefei, Anhui 230027, P.R.China

**Abstract**

The electroweak corrections to the partial widths of the $H^+ \to \tilde{\chi}_i^+ \tilde{\chi}_j^0$ $(i = 1, j = 1, 2)$ decays including one-loop diagrams of the third generation quarks and squarks, are investigated within the Supersymmetric Standard Model. The relative corrections can reach the values about 10%, therefore they should be taken into account for the precise experimental measurement at future colliders.

**PACS: 14.80.Cp, 12.15.Lk, 12.60.Jv, 14.80.Ly**

*Supported by National Natural Science Foundation of China.

Over the past few years, much efforts have been devoted to search the new physics beyond the standard model (SM) [1][2]. The minimal supersymmetric model(MSSM) [3] is considered as one of the most attractive extended models. The MSSM predicts three neutral Higgs bosons, two CP even bosons ($h^0, H^0$) one CP odd boson ($A^0$), and two charged Higgs bosons ($H^{\pm}$). The existence of $H^{\pm}$ bosons would provide conclusive evidence of physics beyond the SM. Therefore, searching for charged Higgs bosons is one of the major tasks at present and future colliders.

In the future Linear Colliders (LC) there are several mechanisms which can produce charged Higgs bosons: (1) Pair production via $e^+e^- \to H^+H^-$ [4] and $e^+e^- \to \gamma\gamma \to H^+H^-$[5]. It is found that these two processes are prominent in discovery of the charged Higgs bosons. (2) Single charged Higgs boson production in association with $W^{\pm}$ gauge boson at $e^+e^-$ colliders, provides an attractive alternative in searching for $H^{\pm}$, which is kinematically favored when $m_{H^{\pm}}$ exceeds $m_W$[6].

At the CERN Large Hadron Collider(LHC), charged Higgs boson pair can be produced via Drell-Yan process $q\bar{q} \to H^+H^-$ [7] and gluon-gluon fusion $gg \to H^+H^-$ at one-loop order[8], when the charged Higgs boson is not too heavy. For a charged Higgs boson with mass $m_{H^{\pm}} < m_t - m_b$, the $H^{\pm}$ bosons can abundantly be produced in decays of top (anti-top) quarks $t(\bar{t}) \to bH^+(\bar{b}H^-)$ from the parent production channel $pp \to t\bar{t}$. The dominant decay channels in this mass range are $H^{\pm} \to \tau^{\pm}\nu_{\tau}$. When $m_{H^{\pm}} > m_t + m_b$, the dominant production of single heavy charged Higgs boson is via $gb(g\bar{b}) \to tH^-(\bar{t}H^+)$ [9], $gg \to t\bar{b}H^-(\bar{t}bH^+)$ [10] and $qb(\bar{q}\bar{b}) \to q'bH^+(\bar{q}'\bar{b}H^+)$[11] processes. The sequential decay $H^+ \to t\bar{b}$ is known as a preferred channel for $H^{\pm}$ boson search. But this charged Higgs

boson signal appears together with large QCD background. Alternative production modes of heavy charged Higgs bosons are associated heavy $H^{\pm}$ production with $W^{\mp}$ bosons via $gg, q\bar{q} \to W^{\pm}H^{\mp}$. In this case the $W^{\pm}$-boson's leptonic decay may be used as a spectacular trigger. This associated heavy $H^{\pm}$ productions with $W^{\mp}$-boson have been investigated in Refs.[12] [13] [14].

The heavy charged Higgs boson decay modes in the SM (including $H^- \to b\bar{t}$,$H^- \to s\bar{c}$,$H^- \to W^-h$ and $H^- \to \tau\bar{\nu_\tau}$) have be studied and simulated in Refs.[15], [16] and the references therein. In Ref.[16] it is concluded that $H^{\pm}$ with mass up to $\sim 400GeV$ can be discovered by the LHC, if $\tan\beta \lesssim 3$ or $\tan\beta \gtrsim 25$. The SUSY decay modes $H^{\pm} \to \tilde{\chi}_i^{\pm}\tilde{\chi}_j^0$ $(i = 1,\ j = 1,2,3)$ as the signatures of the MSSM charged Higgs boson at the LHC have been discussed in Ref.[17], there they simulated the decay $H^{\pm} \to \tilde{\chi}_i^{\pm}\tilde{\chi}_j^0$ $(i = 1,\ j = 1,2,3)$ in the regions of the parameter space, where the identification of $H^{\pm}$ via their SM decay modes have been proven to be ineffective at the LHC. The MSSM decay $H^{\pm} \to \tilde{\chi}_1^{\pm}\tilde{\chi}_1^0$ yields a single hard lepton from the chargino sequential decay, and $H^{\pm} \to \tilde{\chi}_1^{\pm}\tilde{\chi}_2^0$, $(\tilde{\chi}_1^{\pm}\tilde{\chi}_3^0)$ decays yield three leptons from chargino and neutralino decays.

As we know that for the comparison of the theoretical prediction with the precision experiments at the LHC, calculations at tree-level are no more sufficient, the inclusion of radiative corrections is necessary. In this paper, we investigate the one-loop electroweak corrections with top(stop) and bottom(sbottom) contributions to the heavy charged Higgs boson decay $H^{\pm} \to \tilde{\chi}_i^{+}\tilde{\chi}_j^0$ $(i = 1,\ j = 1,2)$. Since there is no one-loop QCD corrections in these processes, so the electroweak corrections with quarks and squarks are most important. The Feynman diagrams for the $H^{\pm} \to \tilde{\chi}_i^{\pm}\tilde{\chi}_j^0$ at the tree-level are shown in figure

1(a). The one-loop Feynman diagrams involving the third generation quarks and their SUSY partners in the decay of charged Higgs boson to chargino and neutralino, are drawn in figures 1(c). The self-energy of charged Higgs boson, chargino self-energy, neutralino self-energy and $H^{\pm} - W^{\pm}$ mixing self-energy are shown in figure 1(d-g) respectively.

In the calculation, we use the t' Hooft gauge and adopt the dimensional reduction scheme(DR)[18], which is commonly used in the calculation of the electroweak correction in frame of the MSSM as it preserves supersymmetry at least at one-loop order, to control the ultraviolet divergences in the virtual loop corrections. The complete on-mass-shell scheme [19][20] is used in doing renormalization.

Firstly, we review briefly the chargino, neutralino, and squark sectors of the MSSM to settle the conventions. The tree-level mass matrices for chargino and neutralino can be expressed below [21]:

$$
\begin{aligned}
X &= \begin{pmatrix} M & \sqrt{2}m_W \sin\beta \\ \sqrt{2}m_W \cos\beta & \mu \end{pmatrix}, \\
Y &= \begin{pmatrix} M^{'} & 0 & -m_Z s_W \cos\beta & m_Z s_W \sin\beta \\ 0 & M & m_Z c_W \cos\beta & -m_Z c_W \sin\beta \\ -m_Z s_W \cos\beta & m_Z c_W \cos\beta & 0 & -\mu \\ m_Z s_W \sin\beta & -m_Z c_W \sin\beta & -\mu & 0 \end{pmatrix}. \qquad (1)
\end{aligned}
$$

Here $s_W \equiv \sin\theta_W, c_W \equiv \cos\theta_W, t_W \equiv \tan\theta_W$. $M$ and $M^{'}$ are the $SU(2)$ and $U(1)_Y$ soft-SUSY-breaking gaugino masses. These matrices can be diagonalized by unitary matrices $U, V, N$ via

$$
\begin{aligned}
U^* X V^{\dagger} &= M_D = \mathrm{diag}\{m_{\tilde{\chi}_1^+}, m_{\tilde{\chi}_2^+}\}, (0 < m_{\tilde{\chi}_1^+} < m_{\tilde{\chi}_2^+}), \\
N^* Y N^{\dagger} &= M_D^0 = \mathrm{diag}\{m_{\tilde{\chi}_1^0}, m_{\tilde{\chi}_2^0}, m_{\tilde{\chi}_3^0}, m_{\tilde{\chi}_4^0}\}, (0 < m_{\tilde{\chi}_1^0} < m_{\tilde{\chi}_2^0} < m_{\tilde{\chi}_3^0} < m_{\tilde{\chi}_4^0}). \quad (2)
\end{aligned}
$$

The tree-level stop and sbottom squared-mass matrices are:

$$\mathcal{M}_{\tilde{t}}^2 = \begin{pmatrix} M_{\tilde{Q}}^2 + m_t^2 + m_Z^2 \cos 2\beta \left(\frac{1}{2} - \frac{2}{3}s_W^2\right) & m_t \left(A_t - \mu \cot\beta\right) \\ m_t \left(A_t - \mu \cot\beta\right) & M_{\tilde{U}}^2 + m_t^2 + \frac{2}{3}m_Z^2 \cos 2\beta s_W^2 \end{pmatrix},$$
$$\mathcal{M}_{\tilde{b}}^2 = \begin{pmatrix} M_{\tilde{Q}}^2 + m_b^2 - m_Z^2 \cos 2\beta \left(\frac{1}{2} - \frac{1}{3}s_W^2\right) & m_b \left(A_b - \mu \tan\beta\right) \\ m_b \left(A_b - \mu \tan\beta\right) & M_{\tilde{D}}^2 + m_b^2 - \frac{1}{3}m_Z^2 \cos 2\beta s_W^2 \end{pmatrix}. \quad (3)$$

The parameters $M_{\tilde{Q}}, M_{\tilde{U}}$ and $M_{\tilde{D}}$ are the soft-SUSY-breaking masses for the third generation SU(2) squark doublet $\tilde{Q} = \left(\tilde{t}_L, \tilde{b}_L\right)$, and the singlets $\tilde{U} = \tilde{t}_R$ and $\tilde{D} = \tilde{b}_R$, respectively. $A_{t,b}$ are the corresponding soft-SUSY-breaking trilinear couplings. We define the squark mass eigenstates as following:

$$\begin{pmatrix} \tilde{q}_1 \\ \tilde{q}_2 \end{pmatrix} = R^{\tilde{q}} \begin{pmatrix} \tilde{q}_L \\ \tilde{q}_R \end{pmatrix}, \quad R^{\tilde{q}} = \begin{pmatrix} \cos\theta_{\tilde{q}} & \sin\theta_{\tilde{q}} \\ -\sin\theta_{\tilde{q}} & \cos\theta_{\tilde{q}} \end{pmatrix}, \quad q = (t, b), \quad (4)$$

$R^{\tilde{q}}$ is used to diagonalize the squark mass matrix $R^{\tilde{q}}\mathcal{M}_{\tilde{q}}^2 R^{\tilde{q}\dagger} = \mathrm{diag}\{\mathrm{m}_{\tilde{\mathrm{q}}_1}^2, \mathrm{m}_{\tilde{\mathrm{q}}_2}^2\}$.

The vertexes of $H^+\tilde{\chi}^+\tilde{\chi}^0$ and $G^+\tilde{\chi}^+\tilde{\chi}^0$, which are related to $H^+ \to \tilde{\chi}_i^+\tilde{\chi}_j^0$ ($i = 1,\ j = 1, 2$) partial decay width are determined by the interaction Lagrangian, which are given by[21]:

$$\mathcal{L}_{H^+\tilde{\chi}^+\tilde{\chi}^0} = -H^+\bar{\tilde{\chi}}_i^+ \left[g \sin\beta Q_{ij}^{\prime R*} P_L + g \cos\beta Q_{ij}^{\prime L} P_R\right] \tilde{\chi}_j^0 + h.c., \quad (5)$$

$$\mathcal{L}_{G^+\tilde{\chi}^+\tilde{\chi}^0} = -G^+\bar{\tilde{\chi}}_i^+ \left[-g \cos\beta Q_{ij}^{\prime R*} P_L + g \sin\beta Q_{ij}^{\prime L} P_R\right] \tilde{\chi}_j^0 + h.c., \quad (6)$$

where$P_{L,R} = \frac{1}{2}(1 \mp \gamma_5)$ are the chirality projection operators, and we denoted:

$$Q_{ij}^{\prime R} = N_{j3}U_{i1} - \sqrt{\frac{1}{2}}(N_{j2} + N_{j1}\tan\theta_W)U_{i2},$$
$$Q_{ij}^{\prime L} = N_{j4}V_{i1} + \sqrt{\frac{1}{2}}(N_{j2} + N_{j1}\tan\theta_W)V_{i2}. \quad (7)$$

The decay width of $H^+ \to \tilde{\chi}_i^+ \tilde{\chi}_j^0$ at the tree-level is expressed as[22]

$$\Gamma_{\rm tree} = \frac{g^2 \lambda^{1/2}}{16\pi m_{H^+}^3} \left[ \left( |F_{ij}^L|^2 + |F_{ij}^R|^2 \right) \left( m_{H^+}^2 - m_{\tilde{\chi}_i^+}^2 - m_{\tilde{\chi}_i^0}^2 \right) - 4 m_{\tilde{\chi}_i^+} m_{\tilde{\chi}_j^0} Re \left( F_{ij}^L F_{ij}^R \right) \right], \tag{8}$$

where

$$\begin{aligned} \lambda^{1/2} &= \left[ \left( m_{H^+}^2 - m_{\tilde{\chi}_i^+}^2 - m_{\tilde{\chi}_j^0}^2 \right)^2 - 4 m_{\tilde{\chi}_i^+}^2 m_{\tilde{\chi}_j^0}^2 \right]^{1/2}, \\ F_{ij}^R &= \sin\beta Q_{ij}^{\prime R}, \qquad F_{ij}^L = \cos\beta Q_{ij}^{\prime L}. \end{aligned} \tag{9}$$

To obtain the renormalized vertex $H^+ \tilde{\chi}_i^+ \tilde{\chi}_j^0$, we introduce parameters and field renormalization constants as follow[19, 20]:

$$\begin{aligned} g &\to \left( 1 + \frac{\delta g}{g} \right) g = \left( 1 + \delta Z_e - \frac{\delta s_W}{s_W} \right) g, \\ \tan\beta &\to \left( 1 + \frac{\delta \tan\beta}{\tan\beta} \right) \tan\beta, \quad t_W \to \left( 1 + \frac{\delta t_W}{t_W} \right) t_W, \\ \begin{pmatrix} H^\pm \\ G\pm \end{pmatrix} &\to \begin{pmatrix} 1 + \frac{1}{2}\delta Z_{H^\pm} & \frac{1}{2}\delta Z_{H^\pm G^\pm} \\ \frac{1}{2}\delta Z_{G^\pm H^\pm} & 1 + \frac{1}{2}\delta Z_{G^\pm} \end{pmatrix} \begin{pmatrix} H^\pm \\ G^\pm \end{pmatrix} \\ \tilde{\chi}_i^+ &\to \left( \delta_{ik} + \frac{1}{2}\delta Z_{+,ik}^L P_L + \frac{1}{2}\delta Z_{+,ik}^R P_R \right) \tilde{\chi}_k^+, \\ \tilde{\chi}_i^0 &\to \left( \delta_{ik} + \frac{1}{2}\delta Z_{0,ik}^L P_L + \frac{1}{2}\delta Z_{0,ik}^R P_R \right) \tilde{\chi}_k^0, \\ U &\to U + \delta U, \quad V \to V + \delta V, \quad N \to N + \delta N, \end{aligned} \tag{10}$$

here for the charged Higgs boson, chargino and neutralino, we introduced the mixed field renormalization constants and the counterterms for the $U$, $V$ and $N$ matrices.

In the on-mass-shell scheme the renormalization constants defined in Eq.(10) can be fixed by the following renormalization conditions[19][20]:

- The renormalized tadpoles, i.e. the sum of tadpole diagrams $T_{h,H}$ and tadpole counter-terms $\delta_{h,H}$ vanish:

$$T_h + \delta t_h = 0, \quad T_H + \delta t_H = 0\,.$$

So no tadpole needed to be considered in our calculation.

- On shell condition for the charged Higgs boson,

$$\tilde{Re}\hat{\Sigma}_{H^\pm H^\pm}(m^2_{H^+}) = 0, \quad \tilde{Re}\hat{\Sigma}'_{H^\pm H^\pm}(m^2_{H^+}) = 0, \tag{11}$$

the "hat" denotes the renormalized quantities, $\Sigma'(m^2) \equiv \frac{\partial\Sigma(p^2)}{\partial p^2}|_{p^2=m^2}$. $\tilde{Re}$ takes only the real part of the loop integrals appearing in the self-energies. From which we abtain

$$\delta m^2_{H^\pm} = \tilde{Re}\Sigma_{H^\pm H^\pm}(m^2_{H^+}), \quad \delta Z_{H^\pm} = -\tilde{Re}\Sigma'_{H^\pm H^\pm}(m^2_{H^+}). \tag{12}$$

- The fermion one-loop renormalized two-point function can be decomposed as

$$i\hat{\Gamma}^f_{ij}(p) = i\delta_{ij}(\not{p} - m_{f_i}) + i\left[\not{p}P_L\hat{\Sigma}^L_{ij}(p^2) + \not{p}P_R\hat{\Sigma}^R_{ij}(p^2) + P_L\hat{\Sigma}^{SL}_{ij}(p^2) + P_R\hat{\Sigma}^{SR}_{ij}(p^2)\right]. \tag{13}$$

$\hat{\Sigma}^{L,R,SL,SR}_{ij}$ are the fermions self-energy matrices. By imposing the on-shell renormalization conditions for fermions, We can obtain the renormalization constants as following:

$$\begin{aligned}
\delta m_i &= \frac{1}{2}\tilde{Re}\left[m_i(\Sigma^L_{ii}(m^2_i) + \Sigma^R_{ii}(m^2_i)) + \Sigma^{SL}_{ii}(m^2_i) + \Sigma^{SR}_{ii}(m^2_i)\right], \\
\delta Z^L_{ii} &= -\tilde{Re}\left[\Sigma^L_{ii}(m^2_i) + m^2_i(\Sigma^{L'}_{ii}(m^2_i) + \Sigma^{R'}_{ii}(m^2_i)) + m_i(\Sigma^{SL'}_{ii}(m^2_i) + \Sigma^{SR'}_{ii}(m^2_i))\right], \\
\delta Z^R_{ii} &= -\tilde{Re}\left[\Sigma^R_{ii}(m^2_i) + m^2_i(\Sigma^{L'}_{ii}(m^2_i) + \Sigma^{R'}_{ii}(m^2_i)) + m_i(\Sigma^{SL'}_{ii}(m^2_i) + \Sigma^{SR'}_{ii}(m^2_i))\right],
\end{aligned}$$

$$
\begin{aligned}
\delta Z^L_{ij} &= \frac{2}{m_i^2 - m_j^2}\tilde{Re}\left[m_j^2\Sigma^L_{ij}(m_j^2) + m_i m_j \Sigma^R_{ij}(m_j^2) + m_i\Sigma^{SL}_{ij}(m_j^2) + m_j\Sigma^{SR}_{ij}(m_j^2)\right], \quad \text{for i} \neq \text{j} \\
\delta Z^R_{ij} &= \frac{2}{m_i^2 - m_j^2}\tilde{Re}\left[m_i m_j \Sigma^L_{ij}(m_j^2) + m_j^2\Sigma^R_{ij}(m_j^2) + m_j\Sigma^{SL}_{ij}(m_j^2) + m_i\Sigma^{SR}_{ij}(m_j^2)\right]. \quad \text{for i} \neq \text{j}
\end{aligned}
\tag{14}
$$

Then we can obtain the chargino wave function renormalization constants $\delta Z_{+,ij}$ and neutralino wave function renormalization constants $\delta Z_{0,ij}$ from above equations.

- The renormalization constant for the electric charge and counterterms of gauge boson masses:

$$
\begin{aligned}
\delta Z_e &= -\frac{1}{2}\delta Z_{\gamma\gamma} - \frac{s_W}{c_W}\frac{1}{2}\delta Z_{Z\gamma} = \frac{1}{2}\Sigma^{T'}_{\gamma\gamma}(0) - \frac{s_W}{c_W}\frac{\Sigma^T_{\gamma Z}(0)}{m_Z^2}, \\
\delta m_V^2 &= \tilde{Re}\Sigma^T_{VV}(m_V^2), \quad (V = W^\pm, Z).
\end{aligned}
\tag{15}
$$

For the weak mixing angle we use the definition $\cos^2\theta_W = \frac{m_W^2}{m_Z^2}$, this gives:

$$
\frac{\delta c_W}{c_W} = \frac{1}{2}\left(\frac{\delta m_W^2}{m_W^2} - \frac{\delta m_Z^2}{m_Z^2}\right). \tag{16}
$$

- The tree level Lagrangian contains a mixing of the gauge boson fields $W^\pm$ and the Goldstone boson fields $G^\pm$, namely

$$
\mathcal{L}_{GW} = i m_W W^-_\mu \partial^\mu G^+ + h.c.. \tag{17}
$$

After substituting the renormalization transformation for the Goldstone defined in Eq.(10), We can obtain the relevant counterterms

$$
\delta\mathcal{L}_{HW} = \frac{1}{2}\delta Z_{G^+H^+} i m_W W^-_\mu \partial^\mu H^+ + h.c.. \tag{18}
$$

Then the renormalized one-particle-irreducible two-point Green function can be written as:

$$i\hat{\Gamma}^{\mu}_{HW}(k) = i\left(\Sigma_{H^+W^+}(k^2) + \frac{1}{2}m_W\delta Z_{G^+H^+}\right)k^{\mu}. \tag{19}$$

We impose the renormalization condition in a way that the physical charged Higgs boson dose not mix with the physical $W$ boson, then we have

$$\tilde{Re}\hat{\Gamma}_{HW}(k)|_{k^2=m^2_{H^+}} = 0 \Longrightarrow \delta Z_{G^+H^+} = \frac{-2\tilde{Re}\Sigma_{H^+W^+}(m^2_{H^+})}{m_W}. \tag{20}$$

If we impose $\delta v_1/v_1 = \delta v_2/v_2$, analogous to the Eq.(A.15) of Ref.[23], We have:

$$\frac{\delta\tan\beta}{\tan\beta} = -\frac{1}{m_W\sin 2\beta}\tilde{Re}\Sigma_{H^+W^+}(m^2_{H^+}), \tag{21}$$

then the counterterm $\delta\tan\beta$ can also be obtain from the $H^+ - W^+$ mixing self-energy.

- The counterterms $\delta U, \delta V$ and $\delta N$ can be fixed by requiring that the counterterms $\delta U, \delta V$, and $\delta N$ cancel the antisymmetric parts of the wave function corrections [23][24][25]:

$$\begin{aligned}
\delta U &= \frac{1}{4}\left(\delta Z^R_+ - \delta Z^{R\dagger}_+\right)U, \\
\delta V &= \frac{1}{4}\left(\delta Z^L_+ - \delta Z^{L\dagger}_+\right)V, \\
\delta N &= \frac{1}{4}\left(\delta Z^L_0 - \delta Z^{L\dagger}_0\right)N.
\end{aligned} \tag{22}$$

The explicit expressions of all the self-energies concerned in our calculation, can be found in the Appendix and the cited references therein.

By substituting Eq.(10) into the bare Lagrangian Eq.(5), we can obtain the counterterms as follow:

$$\begin{aligned}
\delta\mathcal{L}_{H^+\tilde{\chi}^+\tilde{\chi}^0} &\equiv -H^+\bar{\tilde{\chi}}_i^+\left[\delta C_{ij}^L P_L + \delta C_{ij}^R P_R\right]\tilde{\chi}_j^0 \\
&= -H^+\bar{\tilde{\chi}}_i^+\left\{g\sin\beta\left[Q_{ij}^{\prime R*}\left(\delta Z_e - \frac{\delta s_W}{s_W} + \frac{\delta\sin\beta}{\sin\beta} + \frac{1}{2}\delta Z_{H^+} - \frac{1}{2}\cot\beta\delta Z_{G^+H^+}\right)\right.\right. \\
&+ \left.\sum_{k=1}^{2}\frac{1}{2}Q_{kj}^{\prime R*}\delta Z_{+,ki}^R + \sum_{k=1}^{4}\frac{1}{2}Q_{ik}^{\prime R*}\delta Z_{0,kj}^L + \delta Q_{ij}^{\prime R*}\right]P_L \\
&+ g\cos\beta\left[Q_{ij}^{\prime L}\left(\delta Z_e - \frac{\delta s_W}{s_W} + \frac{\delta\cos\beta}{\cos\beta} + \frac{1}{2}\delta Z_{H^+} + \frac{1}{2}\tan\beta\delta Z_{G^+H^+}\right)\right. \\
&+ \left.\left.\sum_{k=1}^{2}\frac{1}{2}Q_{kj}^{\prime L}\delta Z_{+,ki}^L + \sum_{k=1}^{4}\frac{1}{2}Q_{i,k}^{\prime L}\delta Z_{0,kj}^R + \delta Q_{ij}^{\prime L}\right]P_R\right\}\tilde{\chi}_j^0, \qquad (23)
\end{aligned}$$

where we have defined

$$\begin{aligned}
\delta Q_{ij}^{\prime R} &= \delta N_{j3}U_{i1} + N_{j3}\delta U_{i,1} - \frac{1}{\sqrt{2}}\left(\delta N_{j2} + \delta N_{j1}t_W + N_{j1}\delta t_W\right)U_{i,2} - \frac{1}{\sqrt{2}}\left(N_{j2} + N_{j1}t_W\right)\delta U_{i2}, \\
\delta Q_{ij}^{\prime L} &= \delta N_{j4}V_{i1} + N_{j4}\delta V_{i,1} + \frac{1}{\sqrt{2}}\left(\delta N_{j2} + \delta N_{j1}t_W + N_{j1}\delta t_W\right)V_{i,2} + \frac{1}{\sqrt{2}}\left(N_{j2} + N_{j1}t_W\right)\delta V_{i2}.
\end{aligned} \qquad (24)$$

Then the renormalized one-loop part of the amplitude for the decay $H^+ \to \tilde{\chi}_i^+\tilde{\chi}_j^0$ can be written as

$$\mathcal{M}_{ij}^{Loop} = -iH^+\bar{\tilde{\chi}}_i^+\left[C_{ij}^L P_L + C_{ij}^R P_R\right]\tilde{\chi}_j^0; \quad C_{ij}^{L,R} = \delta C_{ij}^{L,R} + \Lambda_{ij}^{L,R}. \qquad (25)$$

where $\delta C_{ij}^{L,R}$ are defined in Eq.(23), and $\Lambda^{L,R}$ are the form factors contributed by the diagrams in Fig.1.(c), their expressions are listed in the Appendix. We have checked both analytically and numerically that the renormalized amplitude Eq.(25) is ultraviolet finite.

We define the relative correction quantitatively as a ratio of the decay width correction

from one-loop diagrams to the tree-level width:

$$\delta^{ij} = \frac{\Gamma_{\rm total}(H^+ \to \tilde{\chi}_i^+ \tilde{\chi}_j^0) - \Gamma_{\rm tree}(H^+ \to \tilde{\chi}_i^+ \tilde{\chi}_j^0)}{\Gamma_{\rm tree}(H^+ \to \tilde{\chi}_i^+ \tilde{\chi}_j^0)}. \tag{26}$$

Now we turn to the numerical analysis. The SM input parameters are chosen as: $m_t = 174.3\ GeV$,$m_b = 4.3\ GeV$, $m_Z = 91.1882\ GeV$, $m_W = 80.419\ GeV$ and $\alpha_{EW} = 1/128$[26]. The SUSY parameters are taken as follows by default unless otherwise stated. We choose $M_{\tilde{Q}} = M_{\tilde{U}} = M_{\tilde{D}} = A_t = A_b = 200GeV$. The ratio of the vacuum expectation values $\tan\beta$ is set to be 4 or 30 in order to make comparison. The mass of charged Higgs boson $m_{H^\pm} = 250\ GeV$. The physical chargino masses $m_{\tilde{\chi}_1^+}$, $m_{\tilde{\chi}_2^+}$ and the lightest neutralino mass $m_{\tilde{\chi}_1^0}$ are set to be 100 $GeV$, 300 $GeV$ and 60 $GeV$, respectively. Then the fundamental SUSY parameters $M$, $M^{'}$ and $\mu$ in Eq.(1) can be extracted from these input chargino masses, lightest neutralino mass $m_{\tilde{\chi}_1^0}$ and $\tan\beta$. Here we assume $\mu$ has negative sign.

In Fig.2 we plot the relative corrections as functions of $\tan\beta$ for $H^+ \to \tilde{\chi}_1^+ \tilde{\chi}_1^0$ and $H^+ \to \tilde{\chi}_1^+ \tilde{\chi}_2^0$. We can see that the relative electroweak corrections for $H^+ \to \tilde{\chi}_1^+ \tilde{\chi}_1^0$ are always positive, while corrections for $H^+ \to \tilde{\chi}_1^+ \tilde{\chi}_2^0$ decay are negative. The corrections increase as the increment of $\tan\beta$ due to the coupling enhancement at large $\tan\beta$. Quantitatively the relative corrections can reach about 10% and $-8\%$ for $\delta^{11}$ and $\delta^{12}$ respectively when $\tan\beta$ is about 36.

In Fig.3 we present the plot of the relative corrections versus the mass of charged Higgs boson. We can see there are some peaks in the figure, which corresponding to the resonance effects at the positions where $m_{H^\pm}(346.2\ GeV) = m_{\tilde{t}_1}(181.1\ GeV) + m_{\tilde{b}_1}(165.1\ GeV)$, $m_{H^\pm}(419.6GeV) = m_{\tilde{t}_1}(181.1\ GeV) + m_{\tilde{b}_2}(238.5\ GeV)$, $m_{H^\pm}(487.2\ GeV) = m_{\tilde{t}_2}(322.1\ GeV) +$

$m_{\tilde{b}_1}(165.1\ GeV)$ for $\tan\beta = 30$, and $m_{H^\pm}(369.2\ GeV) = m_{\tilde{t}_1}(171.7\ GeV) + m_{\tilde{b}_1}(197.5\ GeV)$, $m_{H^\pm}(383.1\ GeV) = m_{\tilde{t}_1}(171.7\ GeV) + m_{\tilde{b}_2}(211.4\ GeV)$ for $\tan\beta = 4$, respectively. For fixed value of $\tan\beta$, the relative correction is insensitive to the variation of the charged Higgs boson mass in the region between 250 $GeV$ and 450 $GeV$ except around the positions at resonance masses. But there is a sharp peak at the position $m_{H^\pm} = 487.2\ GeV$ due to the resonance effect, and the correction can vary from 8% to −3%.

The relative corrections of $H^+ \to \tilde{\chi}_1^+ \tilde{\chi}_1^0$ versus the lightest chargino mass with $\tan\beta = 4$ and $\tan\beta = 30$ are depicted in figure 4. We can see when $\tan\beta = 4$, the relative correction is about 1% for $m_{\tilde{\chi}_1^+}$ varying from 100 $GeV$ to 180 $GeV$, while when $\tan\beta = 30$, the relative correction decreases from 6.5% to 3.8% with $m_{\tilde{\chi}_1^+}$ increasing in the same range. In Fig.5 we present the correction $H^+ \to \tilde{\chi}_1^+ \tilde{\chi}_1^0$ as a function of the lightest neutralino mass. We can see that the relative corrections is insensitive to the variation of $m_{\tilde{\chi}_1^0}$ for small $\tan\beta$, but for large $\tan\beta$, the correction varies from 3.5% to 7.3% as the lightest neutralino mass running from 50 $GeV$ to 90 $GeV$.

The results in Fig.6, are worked out in the mSUGRA scenario. Of the five mSUGRA input parameters($m_0$, $m_{1/2}$, $A_0$, $\tan\beta$ and sign of $\mu$), we take $m_0 = 200\ GeV$, $m_{1/2} = 150\ GeV$, $A_0 = 300\ GeV$, the sign of $\mu$ is set to be negative, and $\tan\beta$ is running from 2 to 35. In our numerical evaluation to get the low energy scenario from the mSUGRA, the renormalization group equations (RGE's)[27] are run from the weak scale $m_Z$ up to the GUT scale, taking all thresholds into account. We use two-loop RGE's only for the gauge couplings and the one-loop RGE's for the other supersymmetric parameters. The GUT scale boundary conditions are imposed and the RGE's are run back to $m_Z$, again taking

threshold into account. In Fig.6 there is a peak at the position $\tan\beta = 3$ on the curve for $\delta^{12}$, which comes from the resonance effect where $m_{\tilde{t}_1} = m_t + m_{\tilde{\chi}_2^0}$ is satisfied. We can see that the correction is sensitive to $\tan\beta$ in mSUGRA scenario, especially when $\tan\beta$ is located in small or large value regions. The correction is varying from 1.5% to $-3\%$ for $H^+ \to \tilde{\chi}_1^+ \tilde{\chi}_1^0$ and 4% to $-2\%$ for $H^+ \to \tilde{\chi}_1^+ \tilde{\chi}_2^0$ when $\tan\beta$ goes from 2 to 35.

In Summary, we have computed the electroweak corrections to the partial widths of the $H^+ \to \tilde{\chi_i}^+ \tilde{\chi}_j^0$ $(i = 1, j = 1, 2)$ decays including the third generation quark and squark one-loop diagrams within the Minimal Supersymmetric Standard Model. We find that the relative corrections can be sizeable and reach the order of 10% , therefore they should be taken into account in the precise experiment analysis.

**Acknowledgement:** This work was supported in part by the National Natural Science Foundation of China(project number: 19875049, 10005009), the Education Ministry of China and the Ministry of Science and Technology of China.

## Appendix A

In this appendix, we list the self-energies of charged Higgs boson, the mixing self-energy of $H^\pm - W^\pm$ and form factors $\Lambda^{L,R}$ contributed by the one-loop Feynman diagrams (Fig.1(c)). For the self-energies of chargino, neutralino, $W$ gauge boson and $Z$ gauge boson with quarks and squarks in loops, one may refer to Ref.[23], the self-energies of $\gamma$ and its mixing with $Z$ gauge boson with quarks and squarks in loop can be found in [28].

The explicit expressions of Feynman rules we used in our calculation can be found in Ref.[21]. We denote the couplings that chargino, neutralino coupling with quark and

squark in the forms as bellow(The notations are the same as those in Ref.[28]):

$$\begin{aligned}
\bar{b}-\tilde{t}_i-\bar{\tilde{\chi}}_j^+ &: \left(V^{(1)}_{b\tilde{t}_i\tilde{\chi}_j^+}P_L+V^{(2)}_{b\tilde{t}_i\tilde{\chi}_j^+}P_R\right)C, \quad \bar{t}-\tilde{b}_i-\tilde{\chi}_j^+ : V^{(1)}_{t\tilde{b}_i\tilde{\chi}_j^+}P_L+V^{(2)}_{t\tilde{b}_i\tilde{\chi}_j^+}P_R,\\
\bar{b}-\tilde{b}_i-\tilde{\chi}_j^0 &: V^{(1)}_{b\tilde{b}_i\tilde{\chi}_j^0}P_L+V^{(2)}_{b\tilde{b}_i\tilde{\chi}_j^0}P_R, \quad \bar{t}-\tilde{t}_i-\tilde{\chi}_j^0 : V^{(1)}_{t\tilde{t}_i\tilde{\chi}_j^0}P_L+V^{(2)}_{t\tilde{t}_i\tilde{\chi}_j^0}P_R, \qquad \text{(A.1)}
\end{aligned}$$

where $C$ is the charge conjugation operator. The couplings between $H^+$ and quark(squark), and the vertex of $W^\pm$ gauge boson coupling with squarks are denoted as:

$$\begin{aligned}
H^+-\bar{t}-b &: V^{(1)}_{H^+tb}P_L+V^{(2)}_{H^+tb}P_R, \qquad H^+-\tilde{t}_i-\tilde{b}_j: V_{H^+\tilde{t}_i\tilde{b}_j},\\
H^+-H^--\tilde{t}_i-\tilde{t}_j &: V_{H^+H^-\tilde{t}_i\tilde{t}_j}, \qquad H^+-H^--\tilde{b}_i-\tilde{b}_j: V_{H^+H^-\tilde{b}_i\tilde{b}_j},\\
W^--\tilde{t}_i(p_1)-\tilde{b}_j(p_2) &: V_{W\tilde{t}_i\tilde{b}_j}(p_1+p_2)^\mu. \qquad \text{(A.2)}
\end{aligned}$$

The charged Higgs boson self-energy reads:

$$\begin{aligned}
\Sigma_{H^\pm H^\pm} &= \frac{-N_c}{8\pi^2}\Big[\left(V^{(1)}_{H^+tb}V^{(1)*}_{H^+tb}+V^{(2)}_{H^+tb}V^{(2)*}_{H^+tb}\right)\left(-A_0(m_t)+m_b^2B_0(p,m_b,m_t)\right)+p^2B_1(p,m_b,m_t)\Big)\\
&+ \left(V^{(1)}_{H^+tb}V^{(2)*}_{H^+tb}+V^{(1)*}_{H^+tb}V^{(2)}_{H^+tb}\right)m_bm_tB_0(p,m_b,m_t)-\frac{1}{2}\sum_{\alpha,\beta=1}^{2}|V_{H^+\tilde{t}_\alpha\tilde{b}_\beta}|^2B_0(p,m_{\tilde{b}_\beta},m_{\tilde{t}_\alpha})\\
&+ \frac{i}{2}\sum_{\alpha=1}^{2}\left[V_{H^+H^-\tilde{b}_\alpha\tilde{b}_\alpha}A_0(m_{\tilde{b}_\alpha})+V_{H^+H^-\tilde{t}_\alpha\tilde{t}_\alpha}A_0(m_{\tilde{t}_\alpha})\right]\Big]. \qquad \text{(A.3)}
\end{aligned}$$

The $H^\pm-W^\pm$ mixed self-energy contributed by the diagrams in Fig.1(g) is expressed as,

$$\begin{aligned}
\Sigma_{H^\pm W^\pm} &= \frac{igN_c}{8\sqrt{2}\pi^2}\left[m_bV^{(2)}_{H^+ud}(B_0(p,m_b,m_t)+B_1(p,m_b,m_t))+m_tV^{(1)}_{H^+ud}B_1(p,m_b,m_t)\right]\\
&+ \frac{N_c}{16\pi^2}\sum_{\alpha,\beta=1}^{2}V_{H^+\tilde{t}_\alpha\tilde{b}_\beta}V_{W\tilde{t}_\alpha\tilde{b}_\beta}[B_0+2B_1](p,\tilde{t}_\alpha,\tilde{b}_\beta). \qquad \text{(A.4)}
\end{aligned}$$

We decompose the form factors $\Lambda^{L,R}$ contributed by the one-loop Feynman diagrams in Fig.1(c) according to

$$\Lambda^{L,R}=\Lambda^{L,R}_{(1)}+\Lambda^{L,R}_{(2)}+\Lambda^{L,R}_{(3)}+\Lambda^{L,R}_{(4)}, \qquad \text{(A.5)}$$

where $\Lambda^{L,R}_{(i)}$ $(i = 1, 2, 3, 4)$ are the form factors contributed by the diagrams in Fig.1(c1), Fig.1(c2), Fig.1(c3) and Fig.1(c4), respectively.

- For diagram Fig.1(c.1), we introduce the following notations:

$$
\begin{aligned}
F^{(1)}_a &= V^{(2)}_{H^+tb} V^{(2)*}_{t\tilde{b}_\alpha \tilde{\chi}^+_i} V^{(1)}_{b\tilde{b}_\alpha \tilde{\chi}^0_j}, \quad F^{(1)}_b = V^{(1)}_{H^+tb} V^{(1)*}_{t\tilde{b}_\alpha \tilde{\chi}^+_i} V^{(2)}_{b\tilde{b}_\alpha \tilde{\chi}^0_j}, \\
F^{(1)}_c &= V^{(2)}_{H^+tb} V^{(2)*}_{t\tilde{b}_\alpha \tilde{\chi}^+_i} V^{(2)}_{b\tilde{b}_\alpha \tilde{\chi}^0_j}, \quad F^{(1)}_d = V^{(1)}_{H^+tb} V^{(1)*}_{t\tilde{b}_\alpha \tilde{\chi}^+_i} V^{(1)}_{b\tilde{b}_\alpha \tilde{\chi}^0_j}, \\
F^{(1)}_e &= V^{(2)}_{H^+tb} V^{(1)*}_{t\tilde{b}_\alpha \tilde{\chi}^+_i} V^{(1)}_{b\tilde{b}_\alpha \tilde{\chi}^0_j}, \quad F^{(1)}_f = V^{(1)}_{H^+tb} V^{(2)*}_{t\tilde{b}_\alpha \tilde{\chi}^+_i} V^{(2)}_{b\tilde{b}_\alpha \tilde{\chi}^0_j}, \\
F^{(1)}_g &= V^{(2)}_{H^+tb} V^{(1)*}_{t\tilde{b}_\alpha \tilde{\chi}^+_i} V^{(2)}_{b\tilde{b}_\alpha \tilde{\chi}^0_j}, \quad F^{(1)}_h = V^{(1)}_{H^+tb} V^{(2)*}_{t\tilde{b}_\alpha \tilde{\chi}^+_i} V^{(1)}_{b\tilde{b}_\alpha \tilde{\chi}^0_j}. \qquad \text{(A.6)}
\end{aligned}
$$

The form factors $\Lambda^{L/R}_{(1)}$ contributed by diagram Fig.1(c1) are:

$$
\begin{aligned}
\Lambda^{L}_{(1)} &= \frac{-iN_c}{16\pi^2} \sum_{\alpha=1}^{2} \Big[ F^{(1)}_a B_0 - \Big( F^{(1)}_d m_b m_{\tilde{\chi}^+_i} + F^{(1)}_e m_t m_{\tilde{\chi}^+_i} + F^{(1)}_a m^2_{\tilde{\chi}^+_i} + F^{(1)}_b m_{\tilde{\chi}^+_i} m_{\tilde{\chi}^0_j} \Big) C_{11} \\
&- \Big( F^{(1)}_h m_b m_t + F^{(1)}_d m_b m_{\tilde{\chi}^+_i} + F^{(1)}_f m_t m_{\tilde{\chi}^0_j} + F^{(1)}_b m_{\tilde{\chi}^+_i} m_{\tilde{\chi}^0_j} + F^{(1)}_a m^2_{\tilde{b}_\alpha} \Big) C_0 \\
&- \Big( F^{(1)}_a (m^2_{\tilde{\chi}^0_j} - m^2_{\tilde{\chi}^+_i}) + F^{(1)}_c m_b m_{\tilde{\chi}^0_j} + F^{(1)}_f m_t m_{\tilde{\chi}^0_j} - F^{(1)}_d m_b m_{\tilde{\chi}^+_i} - F^{(1)}_e m_t m_{\tilde{\chi}^+_i} \Big) C_{12} \Big], \\
\Lambda^{R}_{(1)} &= \Lambda^{L}_{(1)} (F^{(1)}_a \leftrightarrow F^{(1)}_b, F^{(1)}_c \leftrightarrow F^{(1)}_d, F^{(1)}_e \leftrightarrow F^{(1)}_f, F^{(1)}_g \leftrightarrow F^{(1)}_h), \qquad \text{(A.7)}
\end{aligned}
$$

with $B_0 = B_0(p, m_t, m_b)$, $C_{0,11,12} = C_{0,11,12}(k_1, -p_1, m_{\tilde{b}_\alpha}, m_t, m_b)$.

- For diagram Fig.1(c.2), we define the notations as:

$$
\begin{aligned}
F^{(2)}_a &= V^{(2)}_{H^+tb} V^{(2)*}_{t\tilde{t}_\alpha \tilde{\chi}^0_j} V^{(1)}_{b\tilde{t}_\alpha \tilde{\chi}^+_i}, \quad F^{(2)}_b = V^{(1)}_{H^+tb} V^{(1)*}_{t\tilde{t}_\alpha \tilde{\chi}^0_j} V^{(2)}_{b\tilde{t}_\alpha \tilde{\chi}^+_i}, \\
F^{(2)}_c &= V^{(2)}_{H^+tb} V^{(1)*}_{t\tilde{t}_\alpha \tilde{\chi}^0_j} V^{(1)}_{b\tilde{t}_\alpha \tilde{\chi}^+_i}, \quad F^{(2)}_d = V^{(1)}_{H^+tb} V^{(2)*}_{t\tilde{t}_\alpha \tilde{\chi}^0_j} V^{(2)}_{b\tilde{t}_\alpha \tilde{\chi}^+_i}, \\
F^{(2)}_e &= V^{(2)}_{H^+tb} V^{(2)*}_{t\tilde{t}_\alpha \tilde{\chi}^0_j} V^{(2)}_{b\tilde{t}_\alpha \tilde{\chi}^+_i}, \quad F^{(2)}_f = V^{(1)}_{H^+tb} V^{(1)*}_{t\tilde{t}_\alpha \tilde{\chi}^0_j} V^{(1)}_{b\tilde{t}_\alpha \tilde{\chi}^+_i}, \\
F^{(2)}_g &= V^{(2)}_{H^+tb} V^{(1)*}_{t\tilde{t}_\alpha \tilde{\chi}^0_j} V^{(2)}_{b\tilde{t}_\alpha \tilde{\chi}^+_i}, \quad F^{(2)}_h = V^{(1)}_{H^+tb} V^{(2)*}_{t\tilde{t}_\alpha \tilde{\chi}^0_j} V^{(1)}_{b\tilde{t}_\alpha \tilde{\chi}^+_i}. \qquad \text{(A.8)}
\end{aligned}
$$

Then the form factors contributed by Fig.1(c2) can be obtained from the Eq.(A.7) by doing the following exchanges:

$$\Lambda^{L,R}_{(2)} = \Lambda^{L,R}_{(1)}(F^{(1)} \to F^{(2)}, m_t \leftrightarrow m_b, m_{\tilde{t}_\alpha} \leftrightarrow m_{\tilde{b}_\alpha}). \tag{A.9}$$

- For diagram Fig.1(c3), we denote

$$\begin{aligned} F^{(3)}_a &= V_{H^+\tilde{t}_\alpha\tilde{b}_\beta} V^{(2)*}_{b\tilde{b}_\beta\tilde{\chi}^0_j} V^{(1)}_{b\tilde{t}_\alpha\tilde{\chi}^+_i}, \quad F^{(3)}_b = V_{H^+\tilde{t}_\alpha\tilde{b}_\beta} V^{(1)*}_{b\tilde{b}_\beta\tilde{\chi}^0_j} V^{(2)}_{b\tilde{t}_\alpha\tilde{\chi}^+_i}, \\ F^{(3)}_c &= V_{H^+\tilde{t}_\alpha\tilde{b}_\beta} V^{(1)*}_{b\tilde{b}_\beta\tilde{\chi}^0_j} V^{(1)}_{b\tilde{t}_\alpha\tilde{\chi}^+_i}, \quad F^{(3)}_d = V_{H^+\tilde{t}_\alpha\tilde{b}_\beta} V^{(2)*}_{b\tilde{b}_\beta\tilde{\chi}^0_j} V^{(2)}_{b\tilde{t}_\alpha\tilde{\chi}^+_i}. \end{aligned} \tag{A.10}$$

The form factors from Fig.1(c3) are expressed as

$$\begin{aligned} \Lambda^L_{(3)} &= \frac{iN_c}{16\pi^2} \sum_{\alpha,\beta=1}^{2} \left[ F^{(3)}_a m_b C_0 - F^{(3)}_d m_{\tilde{\chi}^+_i} C_{11} + (F^{(3)}_d m_{\tilde{\chi}^+_i} - F^{(3)}_c m_{\tilde{\chi}^0_j}) C_{12} \right], \\ \Lambda^R_{(3)} &= \Lambda^L_{(3)}(F^{(3)}_a \leftrightarrow F^{(3)}_b, F^{(3)}_c \leftrightarrow F^{(3)}_d), \end{aligned} \tag{A.11}$$

with $C_{0,11,12} = C_{0,11,12}(k_1, -p_1, m_b, m_{\tilde{t}_\alpha}, m_{\tilde{b}_\beta})$.

- For diagram Fig.1(c4), we define

$$\begin{aligned} F^{(4)}_a &= V_{H^+\tilde{t}_\beta\tilde{b}_\alpha} V^{(2)*}_{t\tilde{b}_\alpha\tilde{\chi}^+_i} V^{(1)}_{t\tilde{t}_\beta\tilde{\chi}^0_j}, \quad F^{(4)}_b = V_{H^+\tilde{t}_\beta\tilde{b}_\alpha} V^{(1)*}_{t\tilde{b}_\alpha\tilde{\chi}^+_i} V^{(2)}_{t\tilde{t}_\beta\tilde{\chi}^0_j}, \\ F^{(4)}_c &= V_{H^+\tilde{t}_\beta\tilde{b}_\alpha} V^{(2)*}_{t\tilde{b}_\alpha\tilde{\chi}^+_i} V^{(2)}_{t\tilde{t}_\beta\tilde{\chi}^0_j}, \quad F^{(4)}_d = V_{H^+\tilde{t}_\beta\tilde{b}_\alpha} V^{(1)*}_{t\tilde{b}_\alpha\tilde{\chi}^+_i} V^{(1)}_{t\tilde{t}_\beta\tilde{\chi}^0_j}. \end{aligned} \tag{A.12}$$

Then the form factors contributed by Fig.1(c4) can be expressed as:

$$\Lambda^{L,R}_{(4)} = \Lambda^{L,R}_{(3)}(F^{(3)} \to F^{(4)}, m_t \leftrightarrow m_b, m_{\tilde{t}} \leftrightarrow m_{\tilde{b}}). \tag{A.13}$$

The definitions of the one-loop integrals appearing in the above formulas are adopted from the references[29]. The numerical calculation of the vector and tensor loop integral functions can be traced back to four scalar loop integrals $A_0$, $B_0$, $C_0$, $D_0$ as shown in [30].

## References


[1] S.L. Glashow, Nucl. Phys. 22(1961)579; S. Weinberg, Phys. Rev. Lett. 1(1967)1264; A. Salam, Proc. 8th Nobel Symposium Stockholm 1968, ed. N. Svartholm(Almquist and Wiksells, Stockholm 1968) p.367; H.D. Politzer, Phys. Rep. 14(1974)129.

[2] P.W. Higgs, Phys. Lett 12(1964)132, Phys. Rev. Lett. 13 (1964)508; Phys.Rev. 145(1966)1156; F.Englert and R.Brout, Phys. Rev. Lett. 13(1964)321; G.S. Guralnik, C.R.Hagen and T.W.B. Kibble, Phys. Rev. Lett. 13(1964)585; T.W.B. Kibble, Phys. Rev. 155(1967)1554.

[3] H. E. Haber, G. L. Kane, Phys. Rep. 117(1985) 75.

[4] S. Komamiya, Phys. Rev. **D38** (1988) 2158; A. Brignole et al.in Proceedings of the Workshop on $e^+e^-$ Collisions at 50 GeV The Physics Potential, ed. P.M. Zerwas, DESY 92-123; A.Djouadi, J. Kalinowski, P.M. Zerwas, *ibid* and Z. Phys. C57 (1993) 569; A. Arhrib, M. Capdequi Peyranère and G. Moultaka, Phys. Lett. **B341** (1995) 313; Marco A. Diaz and Tonnis A. ter Veldhuis hep-ph/9501315, DPF94 Proceedings; J. Guasch, W. Hollik and A. Kraft KA-TP-19-1999, hep-ph/9911452; A. Arhrib, and G. Moultaka, Nucl. Phys. **B558** (1999) 3, hep-ph/9808317.

[5] D. Bowser-Chao, K. Cheung, and S. Thomas, Phys. Lett.**B315**, 399 (1993); W.G. Ma, C.S. Li ans L. Han, Phys. Rev. **D53**, 1304 (1996). S.H. Zhu, C.S. Li and C.S. Gao, Phys. Rev. **D58** (1998)055007.

[6] S. Kanemura, Eur. Phys. J. **C17** (2000)473; A. Arhrib, M. C. Peyranere, W. Hollik and G. Moultaka, Nucl. Phys. **B581** (2000)34; F. Zhou, W.G. Ma, Y. Jiang X.Q. Li and L.H. Wan, hep-ph/0106103.

[7] N. G. Deshpande, X. Tata and D. A. Dicus, Phys. Rev. **D29** 1527 (1984); E. Eichten, I. Hinchliffe, K. Lane and C. Quigg, Phys. Mod. Rev. **56**, 579 (1984); **58**, 1065(E) (1986).

[8] D. A. Dicus, J.L. Hewett, C. Kao and T.G. Rizzo, Phys. Rev. **D40** 787(1989); Y. Jiang, W.G. Ma, L. Han, and Z.H. Yu, J. Phys. **G24** 83 (1998); O. Brein and W. Hollik, Eur. Phys. J. **C13** 175 (2000)

[9] J.F.Gunion, H.E. Haber, F.E. Paige, W.-K. Tung and S.S.D. Willenbrock, Nucl. Phys. **B294** (1987) 621.

[10] J.L. Diaz-Cruz and O.A. Sampayo, Phys. Rev. **D50**, (1994)6820.

[11] S. Moretti and K. Odagiri, Phys. Rev. **D55**, (1997)5627.

[12] D.A. Dicus, J.L. Hewett, C. Kao and T.G. Rizzo, Phys. Rev. **D40**, 789 (1989); A.A. Barrientos Bendezu and B.A. Kniehl, Phys. Rev. **D59** (1998)015009; Phys. Rev. **D61**, (2000)097701.

[13] F. Zhou, W.G. Ma, Y. Jiang, L. Han, and L.H. Wan, Phys. Rev. **D63** (2001)015002; O. Brein, S. Kanemura, W. Hollik, Phys. Rev. **D63** (2001)015009.

[14] Y.S. Yang, C.S. Li, L.G. Jin and S.H. Zhu, Phys.Rev. D62 (2000) 095012; O. Brein, S. Kanemura, W. Hollik, hep-ph/0008308.

[15] J. Gunion, Phys. Lett. **B32** 125 (1994); D.J. Miller, S. Moretti, D.P. Roy and W.J. Stirling Phys. Rev. **D61** 055011 (2000); S. Moretti, Phys. Lett. **B481** 49 (2000); ATLAS simulation: K.A. Assamagan and Y. Coadou, Preprint ATL-COM-PHYS-2000-017.

[16] K.A. Assamagan, A. Djouadi, M. Guchait, R. Kinnunen, J.L. Kneur, D.J. Miller, S. Moretti, K. Odagiri and D.P. Roy, Contribution to the works 'Physics at TeV Colliders' Les Houches, France, 8-18 June **1999**, preprint PM/00-03, pages 36-53, February 2000, hep-ph/0002258 (to appear in the proceedings).

[17] M. Bisset, M. Guchait, S. Moretti, DESY-00-150, TUHEP-Th-00124, RAL-TR-2000-029, December 2000.

[18] D.M. Copper, D.R.T. Jones and P. van Nieuwennuizen Nucl. Phys. **B167** 479(1980); W. Siegel, Phys. Lett. **B84** 193(1979).

[19] A. Denner, Fortschr. Phys. **41** (1993) 307.

[20] M. Böhm, H. Spiesberger, W. Hollik, Fortsch. Phys. **34** (1986) 687; W. Hollik, Fortschr. Phys. **38**(1990) 165.

[21] J.F. Gunion, H.E. Haber, Nucl. Phys. **B272**(1986)1.

[22] J.F. Gunion and H.E. Haber, Nucl. Phys. **B307** 445(1988); ibid **B272** 1(1986); Errantum, ibid. **B402** 567(1993).

[23] H. Eberl, M. kincel, W. Majerotto, Y. Yammada, hep-ph/0104109.

[24] A. Denner, T. Sack, Nucl. Phys. **B347**, 203.

[25] B. A. Kniehl, A. Pilaftsis, Nucl. Phys. **B474** (1996) 286.

[26] Particle Data Group, Eur. Phys. J. **C15** 2000.

[27] V. Barger, M. S. Berger and P. Ohmann, Phys. Rev. **D47**, 1093(1993), **D47**, 2038(1993); V. Barger, M. S. Berger, P. Ohmann and R. J. N. Phillips, Phys. Lett. **B314**, 351(1993); V. Barger, M. S. berger and P. Ohmann, Phys. Rev. **D49**, 4908(1994).

[28] M.L. Zhou, W.G. Ma, L. Han, Y. Jiang and H. Zhou, J. Phys. **G25** 1641(1999)

[29] Bernd A. Kniehl, Phys. Rep. **240** 211(1994).

[30] G. Passarino and M. Veltman, Nucl. Phys. **B160**, 151(1979)

**Figure Captions**

**Fig.1** Feynman diagrams including one-loop quark and squark corrections to the decay $H^+ \to \tilde{\chi}_i^+ \tilde{\chi}_j^0$: Fig.1(a) tree-level diagram. Fig.1(b) counterterm for the vertex. Fig.1(c) vertex diagrams, the lower indexes $\alpha, \beta = 1, 2$. Fig.1(d) charged Higgs boson self-energies. Fig.1(e) chargino self-energies. Fig.1(f) neutralino self-energies and Fig.1(g) are the $H^+W^+$ mixing self-energies.

**Fig.2** The relative correction as a function of $\tan\beta$ with $m_{H^+} = 250\ GeV$, $m_{\tilde{\chi}_1^+} = 100\ GeV$, $m_{\tilde{\chi}_2^+} = 300\ GeV$, $m_{\tilde{\chi}_1^0} = 60\ GeV$, and $m_{\tilde{Q}} = m_{\tilde{U}} = m_{\tilde{D}} = A_t = A_b = 200\ GeV$.

**Fig.3** The relative correction as a function of charged Higgs boson mass.

**Fig.4** The relative correction $\delta^{11}$ as a function of the light chargino mass $m_{\tilde{\chi}_1^+}$.

**Fig.5** The relative correction $\delta^{11}$ as a function of the lightest neutralino mass $m_{\tilde{\chi}_1^0}$.

**Fig.6** The relative correction as a function of $\tan\beta$ in mSUGRA scenario.

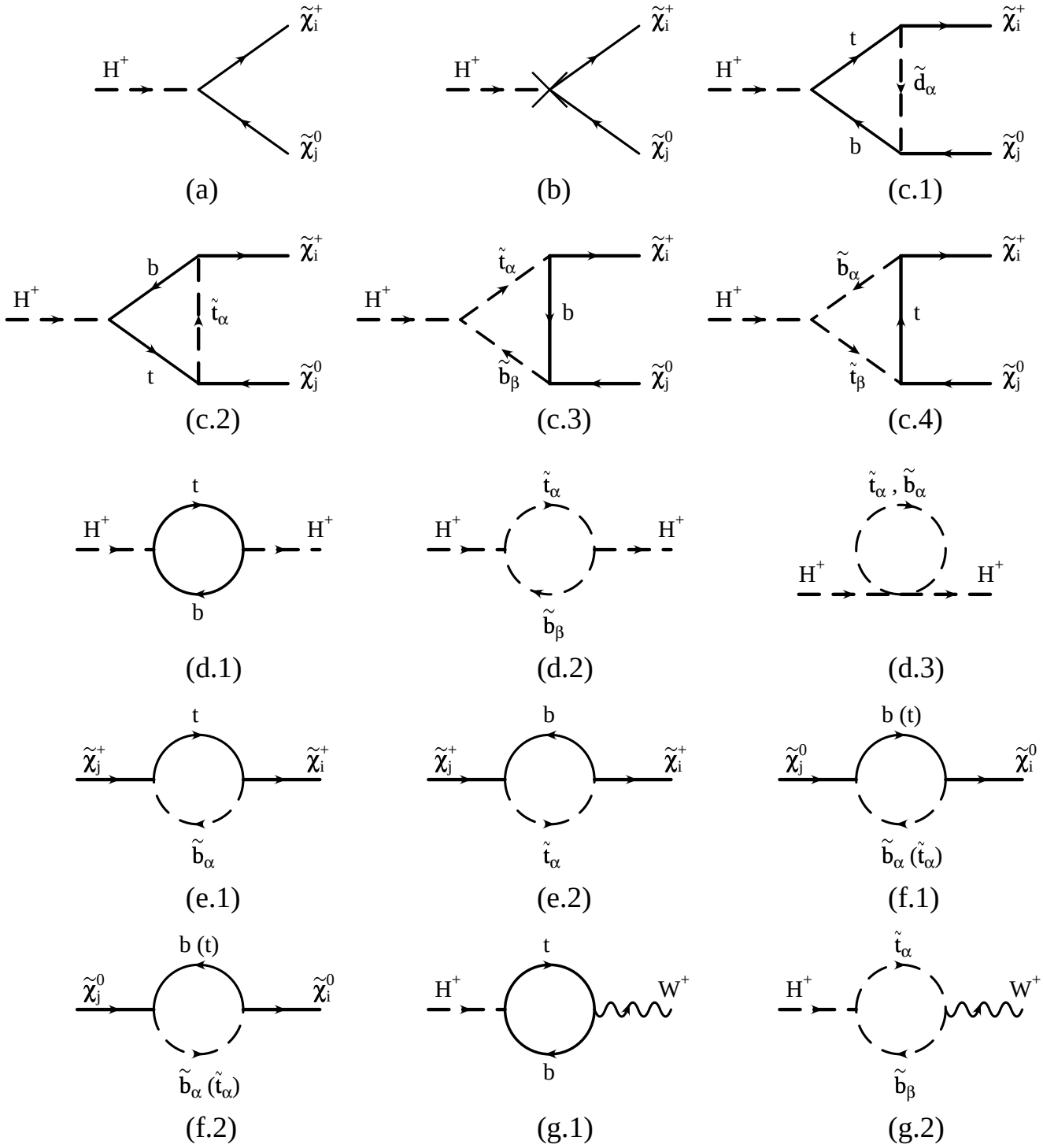
H+
$\tilde{\chi}_i^+$
$\tilde{\chi}_j^0$
(a)
(b)
t
$\tilde{d}_\alpha$
b
(c.1)
$\tilde{t}_\alpha$
(c.2)
$\tilde{b}_\beta$
(c.3)
$\tilde{b}_\alpha$
(c.4)
H+
(d.1)
(d.2)
$\tilde{t}_\alpha$ , $\tilde{b}_\alpha$
(d.3)
$\tilde{\chi}_j^+$
$\tilde{\chi}_i^+$
$\tilde{b}_\alpha$
(e.1)
(e.2)
b (t)
$\tilde{\chi}_j^0$
$\tilde{\chi}_i^0$
$\tilde{b}_\alpha$ ($\tilde{t}_\alpha$)
(f.1)
(f.2)
W+
(g.1)
(g.2)

Figure. 1

Fig.2

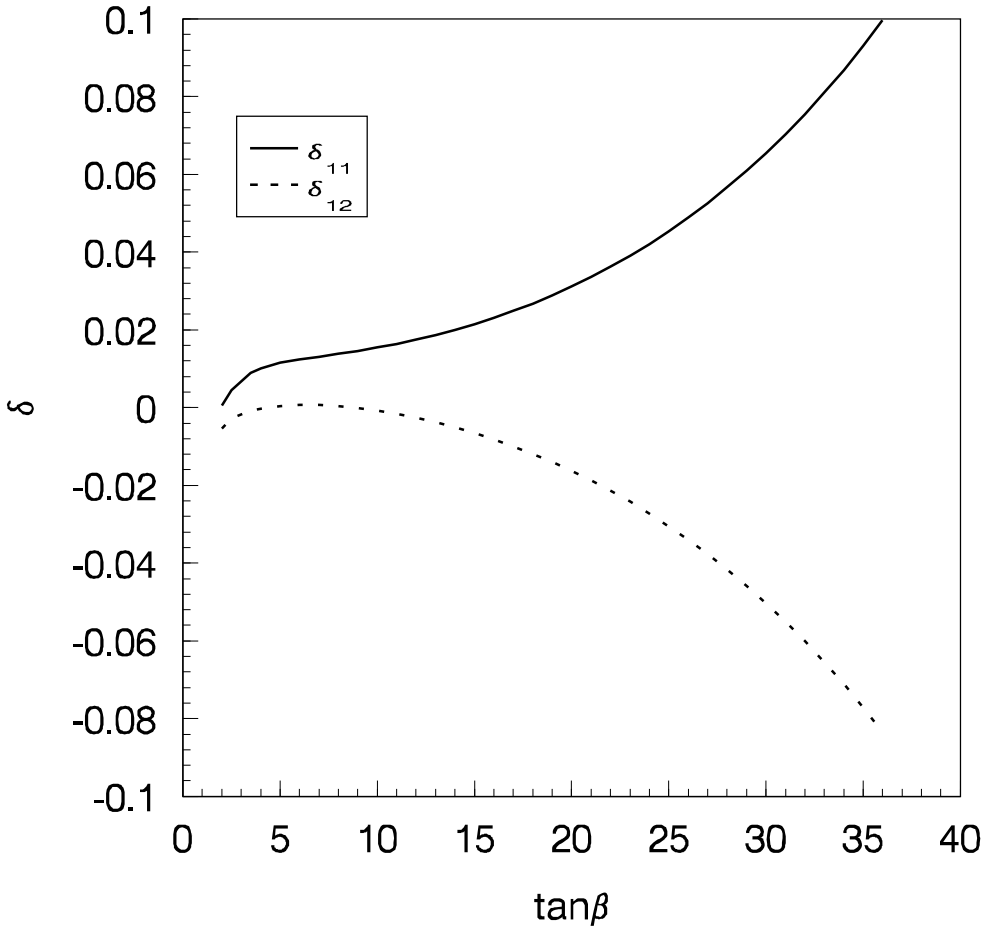
0.1
0.08
0.06
0.04
0.02
0
-0.02
-0.04
-0.06
-0.08
-0.1
δ
δ11
δ12
0
5
10
15
20
25
30
35
40
tanβ

Fig.3

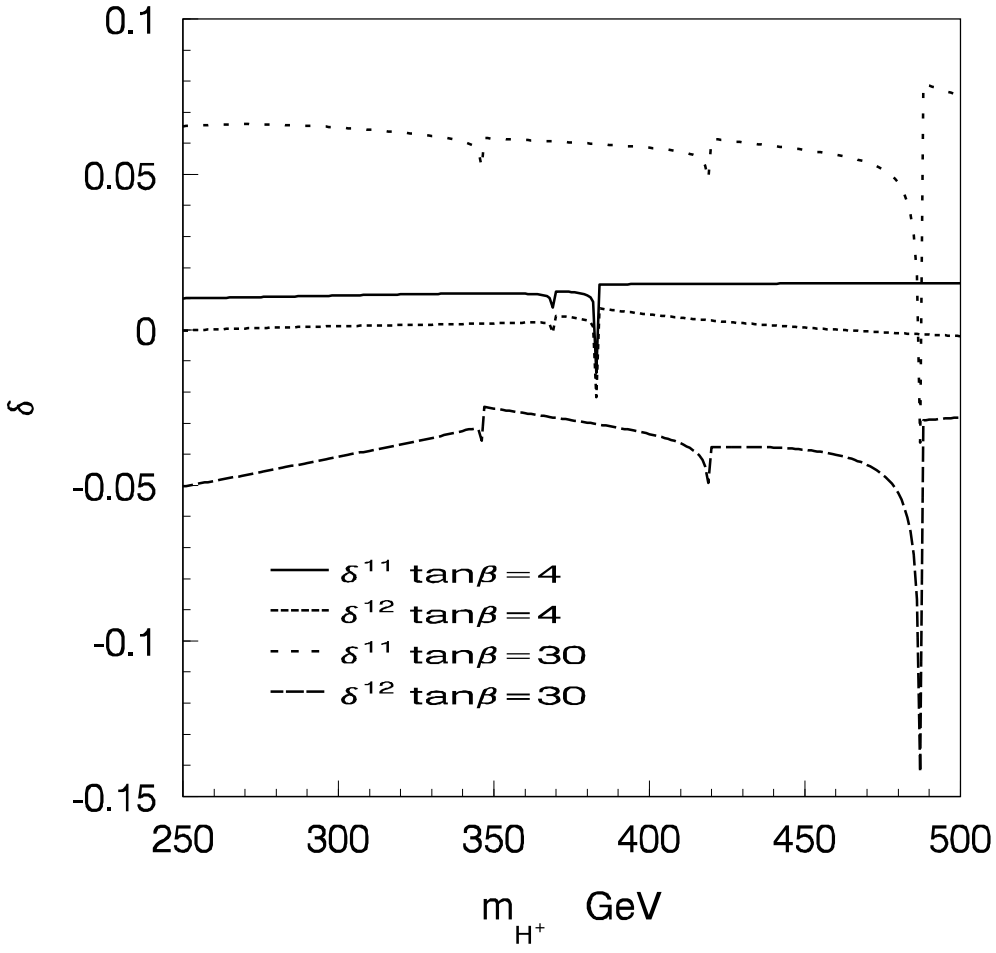
0.1
0.05
0
-0.05
-0.1
-0.15
δ
250
300
350
400
450
500
m H+ GeV
δ11 tanβ=4
δ12 tanβ=4
δ11 tanβ=30
δ12 tanβ=30

Fig.4

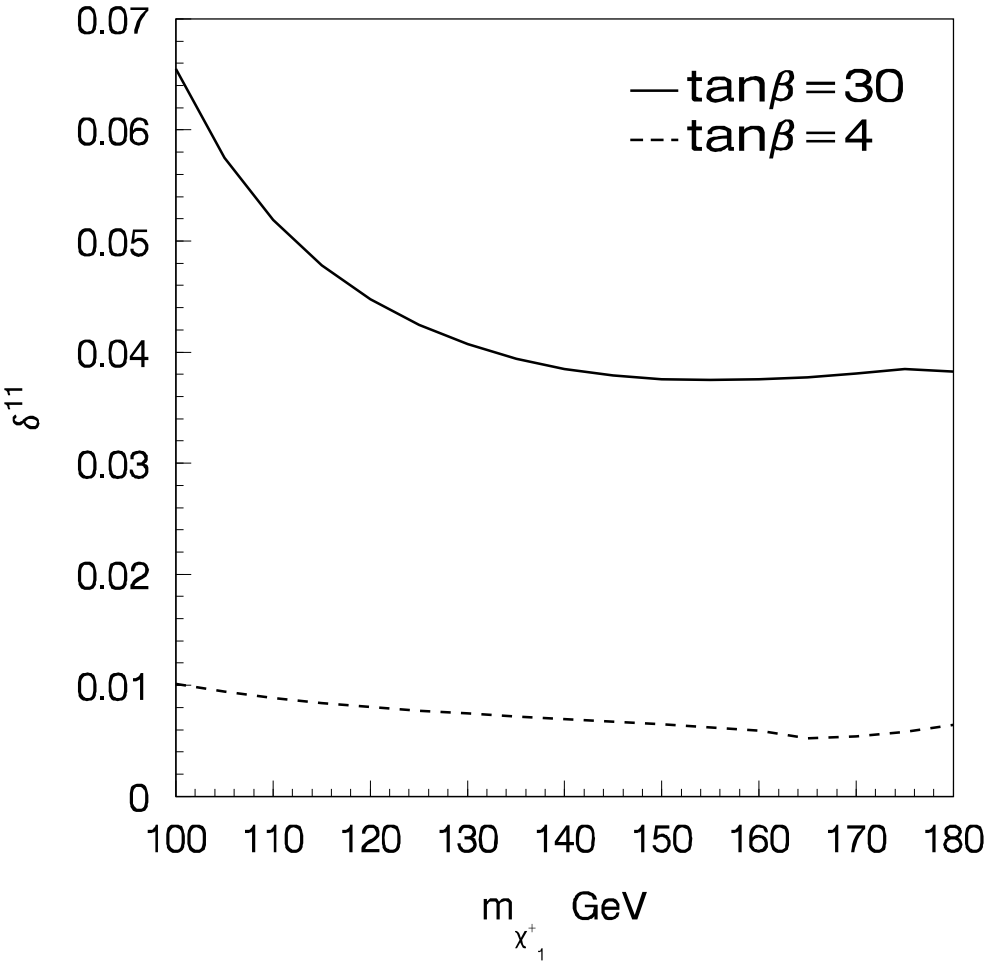
0.07
0.06
0.05
0.04
0.03
0.02
0.01
0
$\delta^{11}$
$\tan\beta = 30$
$\tan\beta = 4$
100
110
120
130
140
150
160
170
180
$m_{\chi^+_1}$ GeV

Fig.5

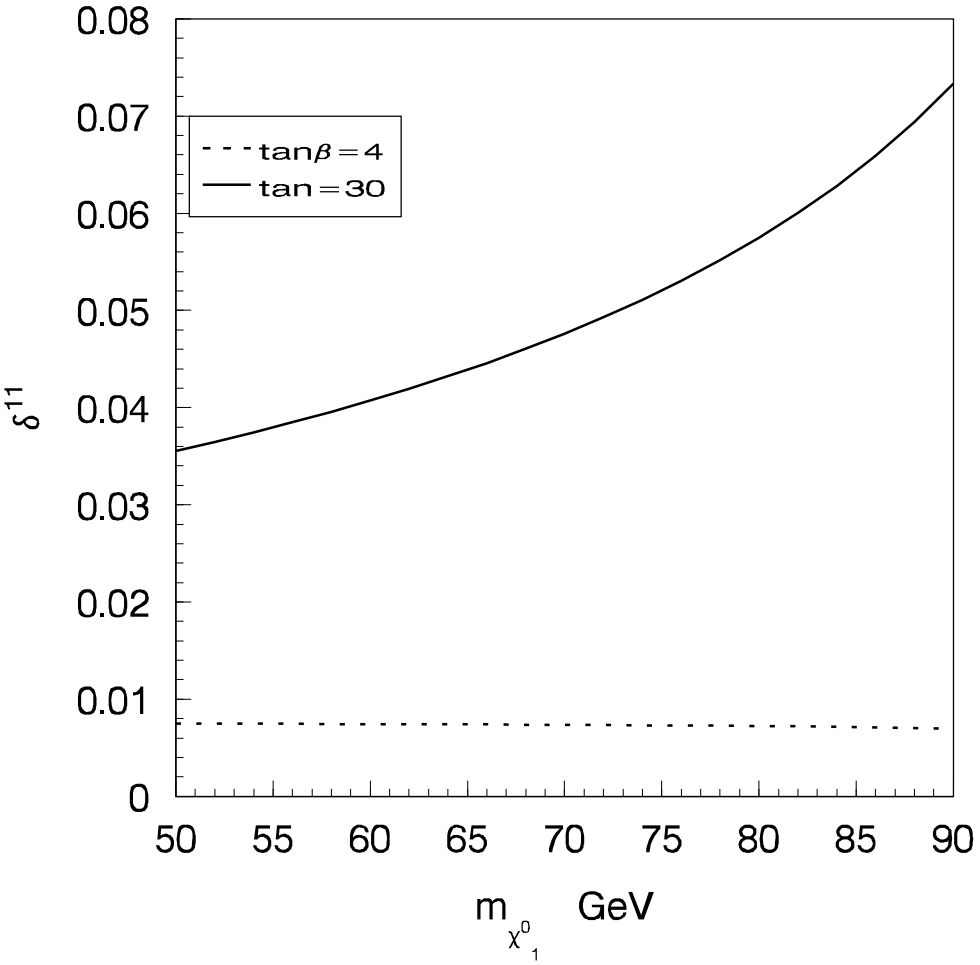
0.08
0.07
0.06
0.05
0.04
0.03
0.02
0.01
0
$\delta^{11}$
tan$\beta$ = 4
tan = 30
50
55
60
65
70
75
80
85
90
$m_{\chi^0_1}$ GeV

Fig.6

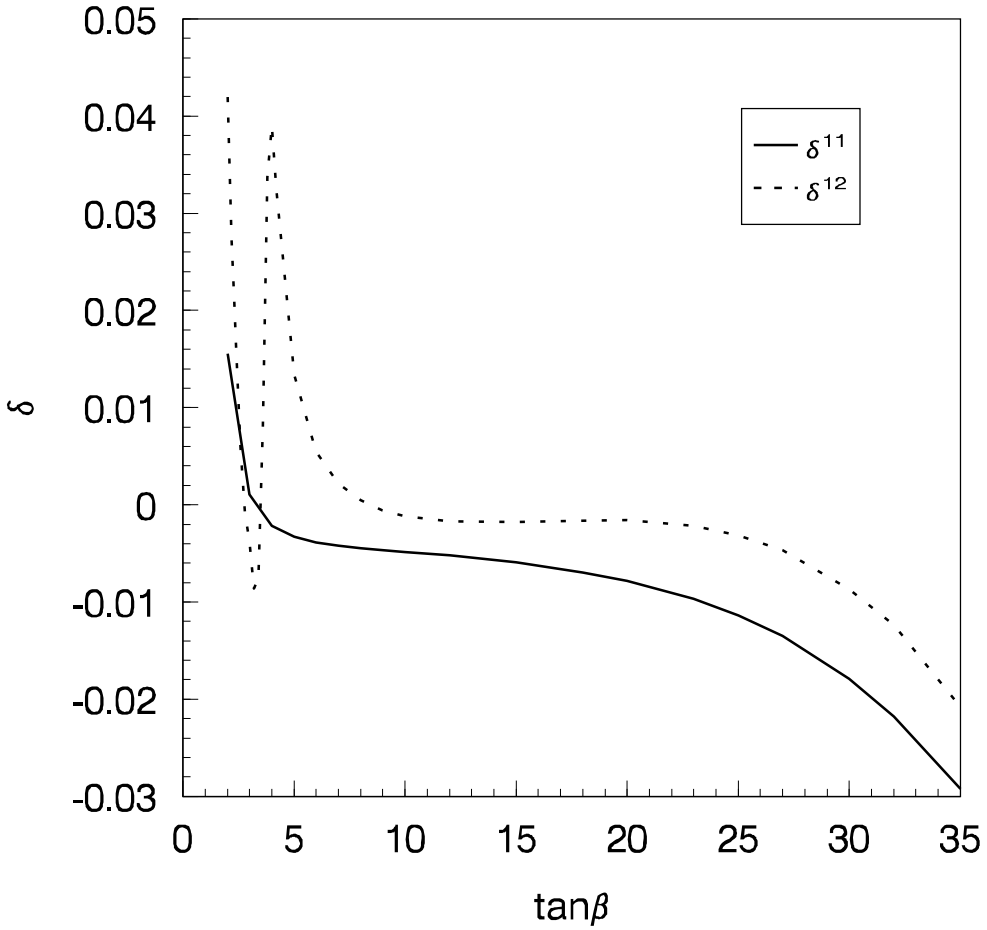
0.05
0.04
0.03
0.02
0.01
0
-0.01
-0.02
-0.03
δ
0
5
10
15
20
25
30
35
tanβ
δ11
δ12